Probing the Anion Binding Promiscuity of the Soluble Nitrate Sensor NreA from *Staphylococcus carnosus*

Ke Ji, Elizabeth K. Pack†, Caden Maydew†, Kevin A. Alberto, Sameera Abeyrathna, Rhiza Lyne E. Villones, Humera Gull, Gabriele Meloni*, Steven O. Nielsen*, and Sheel C. Dodani*

Department of Chemistry and Biochemistry, The University of Texas at Dallas, Richardson, TX 75080

†E.K.P. and C.M. contributed equally.

*sheel.dodani@utdallas.edu, steven.nielsen@utdallas.edu, gabriele.meloni@utdallas.edu

Abstract

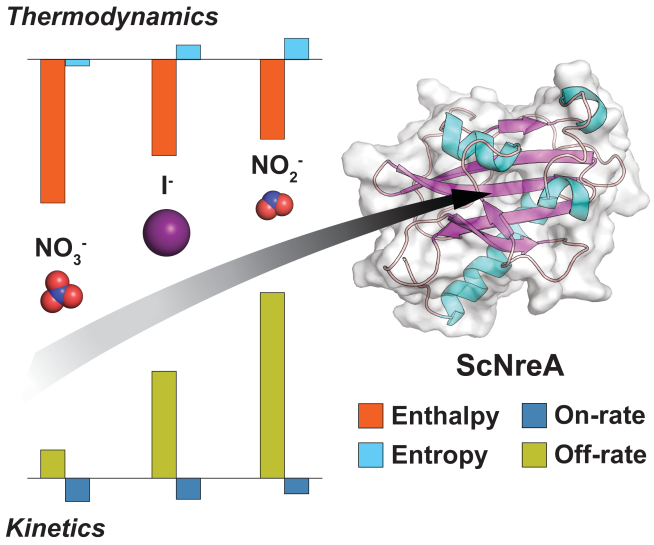

Promiscuity, or selectivity on a spectrum, is an encoded feature in biomolecular anion recognition. To unravel the molecular drivers of promiscuous anion recognition, we have employed a comprehensive approach – spanning experiment and theory – with the *Staphylococcus carnosus* nitrate regulatory element A (ScNreA) as a model. Thermodynamic analysis reveals that ScNreA complexation with native nitrate and nitrite or non-native iodide is an exothermic process. Further deconvolution of the association and dissociation kinetics for each anion reveals that the release event can be limiting, in turn, giving rise to the observed selectivity: nitrate > iodide > nitrite. These conclusions are supplemented with molecular dynamics simulations that capture an entry and exit pathway coupled to subtle global protein motions unique to each anion. Taken together, our data point to how structural plasticity of the binding pocket controls the relative promiscuity of ScNreA to guarantee physiological nitrate sensing.

Introduction

Anion coordination by proteins is of paramount significance for recognition, transformation, and translocation processes in biology.[1–3] From a supramolecular perspective, this is simply driven by patterned cooperative, non-covalent interactions (e.g., arginine residues and backbone amides) combined with the hydrophobic effect.[4] These host design elements are often matched to the intrinsic physical properties of a guest anion including the anion size, shape, charge, basicity, and dehydration enthalpy.[4–7] On this basis, proteins can exhibit an exquisite degree of anion selectivity. Historically, this has been exemplified by comparing the bacterial periplasmic proteins which bind phosphate and sulfate.[8,9] On the other hand, proteins can be promiscuous, resulting in anion selectivity on a spectrum; examples include carbonic anhydrase enzymes and chloride channels.[10,11] Inspired by these curious observations, we have established a program to explore and exploit promiscuity in anion-sensitive fluorescent proteins.[12–16] More recently, we broadened our scope to unravel the molecular drivers of promiscuity versus specificity with underexplored soluble bacterial nitrate receptors as an initial model.[17]

In this regard, we have chosen to work with NreA, a unique nitrate sensory protein found in the food grade bacterium *Staphylococcus carnosus* (ScNreA) (Figure 1A).[18,19] The notion of promiscuity first arose from early-stage phasing with iodide to determine the ScNreA X-ray crystal structure (Figure 1B).[20] ScNreA adopts a GAF_2 domain fold with a binding cleft defined by dipole moments oriented along the α3 and α6 helices.[20] Specifically, three main chain amides connecting residues L67, A68, and I97, and one sidechain amide from residue W45 coordinate to nitrate and iodide. Nearby hydrophobic residues – L61, G66, Y95, P96, and I97 – shield the binding pocket from bulk water.[20]

The second notion of promiscuity arises when considering its biological function. ScNreA is a key component of the nitrate regulatory system NreABC.[21] This controls nitrate-induced anaerobic respiration to generate ammonia via nitrite.[22] Under aerobic conditions and in the absence of nitrate, ScNreA forms a complex with the oxygen sensor kinase NreB.[23] In turn, this prevents phosphorylation of the response regulator NreC and transcription of the nitrate reductase NarG.[21] However, under anaerobic conditions in the presence of nitrate, ScNreA dissociates from NreB, relieving the downstream repression.[23] Similar effects are observed with iodide but not with nitrite, controlling the bacterium's metabolic state.[20] Whether this level of selectivity is solely at the level of ScNreA is unknown.

Building from these observations, ScNreA is ideal for our goal and affords four advantages. One, it is a soluble protein that can be readily expressed recombinantly and purified on a preparative scale from *Escherichia coli*.[20] Two, ScNreA is amenable to analysis of anion binding thermodynamic properties; indeed, Niemann and colleagues previously measured the nitrate binding affinity with isothermal titration calorimetry (ITC).[20] Three, ScNreA has only two tryptophan residues – W45 described above and W112 on a flexible loop facing bulk water.[20] Given this, the intrinsic fluorescence signal of W45 could be used to capture and quantitatively analyze binding kinetics. Four, the X-ray crystal structures are available which

enables studies using molecular dynamics (MD) simulations. To date, no other biophysical insights for ScNreA have been reported. Here, we integrate experimental and *in silico* methods to dissect the interactions of ScNreA with the native nitrate and nitrite and non-native iodide.

Results

Thermodynamic Characterization

We first optimized a method to express and purify ScNreA with a C-terminal polyhistidine tag from *E. coli* (Figures S1, S2). For all experiments, the monomeric form was evaluated at pH 7.8 in 50 mM HEPES buffer with 50 mM NaCl. To quantitatively determine the thermodynamics parameters of nitrate, nitrite, and iodide recognition, ITC was employed at 25, 20, 15, and 10 °C (Figures S3–S8; Tables S1–S6; Table 1). Overall, the three anions interact with ScNreA with similar thermodynamic governing principles. All binding reactions are exothermic and driven by large enthalpic changes (ΔH) with minimal entropic gains (TΔS), except at 25 °C with nitrate. Moreover, the Gibbs free energy change (ΔG) remains relatively constant at each temperature for a given anion. As such, clear differences emerge in the relative binding affinities (K_d). This trend can be ranked from strongest to weakest K_d as follows: nitrate > iodide > nitrite. Of note, our measured binding affinity for nitrate ($K_d \approx 4$ μM) is approximately (*ca.*) 6-fold stronger than that previously reported ($K_d \approx 22$ μM) at 25 °C.[20] We speculate this could arise from differences in ionic strength.

The ΔG for nitrate binding to ScNreA is *ca.* -31.2 kJ/mol (Table 1). In line with the concept of enthalpy-entropy compensation, the enthalpic term increases and the entropic term decreases as the temperature increases.[24] The dependence of ΔH on temperature can be interpreted in terms of a negative heat capacity change upon nitrate binding ($\Delta C_p \approx$ -308.2 J/mol•K, Table S7).[25] Such a value can be linked to protein motions that result in shielding of nonpolar surfaces from bulk water due to increased hydrophobic interactions upon nitrate recognition. Contributions to the total entropy change (ΔS_{total}) can be dissected using a previously established model.[26] At 25 °C, while water release (ΔS_{solv}) is favorable with nitrate, overcompensation by configurational changes (ΔS_{conf}) and restricted motions ($\Delta S_{r/t}$) results in an unfavorable ΔS_{total} of -4.6 J/mol•K (Tables S8, S9).

Next, the ΔG for iodide binding to ScNreA is *ca.* -24.9 kJ/mol (Table 1). This is favorable but translates to a K_d that is weaker than nitrate (Table 1). Interestingly, unlike nitrate, the enthalpy-entropy change is inversely correlated with increasing temperature. This trend grants a positive ΔC_p of *ca.* 242.3 J/mol•K. To our knowledge, this is a rare observation, particularly for an anion binding protein.[27] A positive ΔC_p can be attributed to shielding of polar surfaces, exposing nonpolar surfaces to bulk water.[28] The unique hydration pattern of iodide could also be a contributing factor. Water molecules in the first hydration shell can have stronger interactions with water molecules in the second hydration shell compared to iodide itself.[27,29,30] In line with this, the ΔS_{solv} at 25 °C is unfavorable, likely stemming from

dehydration of iodide, but the ΔS_{conf} contribution at 25 °C dominates, resulting in a favorable ΔS_{total} of 11.1 J/mol•K (Tables S8, S9).

Lastly, consistent with the weakest K_d, the ΔG for nitrite binding to ScNreA is *ca.* -22.7 kJ/mol (Table 1). As observed with iodide, ΔH decreases and TΔS increases to compensate as temperature increases but over a narrower range. The absolute value for ΔC_p is *ca.* 33.1 ± 11.2 J/mol•K, but the analysis of the uncertainty indicates that ΔC_p fluctuates around zero (Table S7). While this suggests that there is little to no change in shielding of the protein surface area, it does not necessarily indicate an absence of a conformational change.[31] Looking to the ΔS_{total} of 16.1 J/mol•K, the ΔS_{solv} contribution is negligible whereas the ΔS_{conf} is favorable (Tables S8, S9).

Kinetic Characterization

Building from the thermodynamic insights, we next probed if and how characteristics of association and dissociation kinetic properties could contribute to anion recognition by ScNreA. The intrinsic fluorescence signal of W45 at λ_{em} = 305 nm was monitored using time-resolved stopped-flow fluorescence emission spectroscopy for the binding of ScNreA with nitrate, iodide, and nitrite.[32] To maximize the signal-coverage acquisition for rapid association and dissociation events, all measurements were carried out at 10 °C. Under pseudo-first order conditions, a rapid, concentration-dependent fluorescence quenching is observed for each anion (Figures S9–S16; Table 2).

Each kinetic trace was fitted to a single exponential model to determine the observed apparent association rate constants (k_{obs}).[33] From the linear dependency of k_{obs} as a function of anion concentration, supporting simple 1:1 association events, linear regression fitting was used to extrapolate the absolute association rate constant (k_{on}) from the slope and the absolute dissociation rate constant (k_{off}) from the y-intercept.[33] Tracking with the K_d, the k_{on} can be ranked from fastest to slowest as follows: nitrate > iodide > nitrite; whereas the trend for k_{off} is reversed: nitrate < iodide < nitrite (Table 2). These data indicate a greater contribution of the anion dissociation rates to the observed differences in K_d.

On the extreme ends, the k_{off} for nitrate is *ca.* 7-fold slower than nitrite. To validate the magnitude of the absolute dissociation rate constant (k_{off}) determined from complex-formation kinetics, apparent dissociation rates ($k_{off\text{-}observed}$) were directly determined form dissociation-by-dilution stopped-flow experiments. While this was only possible for the nitrate-ScNreA complex (Figures S17, S18), due to the very rapid dissociation kinetics for nitrate and iodide, the magnitude of the determined $k_{off\text{-}observed}$ (Table S10) are consistent with the determined absolute nitrate dissociation rate constant (Table 2).

In silico Characterization

Finally, we employed an *in silico* approach to uncover the molecular basis for the experimental differences observed between each anion.[34] MD simulations were performed

at 20 °C with a reconstructed, full-length ScNreA in the apo, nitrate, iodide, and nitrite bound states. Throughout the trajectories, distances were measured between the coordinating residue (W45) and backbone amides (connecting G66 and L67; L67 and A68; P96 and I97) (Figure 1; Figures S19–S22). In the absence of any constraints, all three anions can leave and re-enter the binding pocket through the same pathway, albeit with varying frequencies and resident times. Notably, the nitrite bound form is only observed in *ca.* 2% of the frames. Upon closer examination of the protein surface, there is a tendency for the anions to interact with electropositive regions that are composed primarily of arginine and lysine (Figure S23). While this observation is unsurprising, analysis of anion occupancy near the binding pocket reveals a point of entry, which is most apparent with nitrate and iodide (Figure 3; Figure S24; Supporting Movies 1–3). Thus, the following conjectures are based on these two anions.

In the apo form, the electropositive sidechains of R62 and K65 face outward into the bulk water, serving as an attractive anchor (Figure 3, apo panel). Upon anion (re-)entry, the side chain of R62 can rotate inward, and along with the backbone amide connecting L61 and R62, it can directly engage with the anion (Figure 3, phase 1 panel; Supporting Movie 2). Following this, the sidechain of W45 and the backbone amide connecting P96 and I97 form new interactions (Figure 3, phase 2 panel; Supporting Movies 1, 3), drawing the anion further into the binding pocket. In the fully bound state, these backbone amides on the alpha helices α3 and α6 directly coordinate to the anion (Figure 3, bound panel).

While surrounding nonpolar residues (e.g., L61, Y95, V98) are needed to promote and maintain the hydrophobic effect, water molecules can still penetrate the binding pocket. They can transiently coordinate, and even bridge nearby residues (e.g., W45) or backbone amides (e.g., P96 and I97) to the anion (Supporting Movies 1, 3; Figure S25). Even though these observations can be generalized for both nitrate and iodide, the ScNreA coordination sphere is dynamic and unique for each anion. This is supported by the frequency of interactions during the trajectories (Figure S26). On the extreme ends, W45 prefers nitrate over iodide, whereas the backbone amide connecting I97 and V98 prefers iodide over nitrate.

To understand how ScNreA could register anion binding at the per residue level, we next used a root mean square fluctuation (RMSF) analysis.[35,36] The most dynamic residues (ΔRMSF ≥ 1 Å or ≤ -1 Å) are found in flexible loops (Figure S27). Of these, residues spanning 84 to 94 can form a disordered loop or an alpha helix during the simulations, but only the latter is apparent in the original crystal structures. With respect to apo ScNreA, the RMSF of residues 59–63 and 84–88 with nitrate show a large increase (up to 4 Å), whereas the RMSF of residues 84–94 with iodide shows a large decrease (up to 4 Å). Further analysis with dynamic cross-correlation (DCC) shows correlated motions upon anion binding.[37] While no differences are observed for nitrate, a clear reduction is observed with iodide (Figures S28–S30).

These changes in protein motion are further reinforced by the solvent-accessible surface area (SASA) calculations.[38] Little to no differences are observed in the absence or presence of anion (SASA ≈ 9894 Å^2) with the exception that ScNreA can adopt an additional, less solvent-

exposed state with iodide (SASA ≈ 9107 Å^2, Figure S31). Finally, principal component analysis (PCA) reveals the global conformations for each ScNreA state (Figures S32–S34).[39] Apo ScNreA samples a wider, spatially distinct conformational space relative to both anion bound states, which are distinct themselves.

Discussion

In summary, we have investigated how the soluble sensor NreA from *Staphylococcus carnosus* can recognize not only the native nitrate and nitrite but also non-native iodide. Our calorimetric analyses reveal that anion complexation with ScNreA is an exothermic process with enthalpy as the key driving force. When comparing the binding affinities for all three anions, a clear preference emerges. ScNreA favors nitrate up to *ca.* 19-fold and 51-fold over iodide and nitrite, respectively. Moreover, anion binding is not rate limiting. In fact, it is a fast process that occurs on the millisecond timescale. While differences can be measured in the on-rate, these are significantly amplified by the off-rate. The ScNreA-nitrate complex dissociates *ca.* 4-fold and 7-fold slower than iodide and nitrite, respectively, suggesting that dissociation kinetics governs anion selectivity.

This promiscuous anion recognition is coupled to conformational plasticity of ScNreA. Experimentally, the change in heat capacity reflects differential global protein motions, leading to shielding and exposure of nonpolar surfaces to water for nitrate and iodide, respectively, or no difference for nitrite. Since the binding site is conserved, it is plausible that each anion complex could exist in a conformational equilibrium between more than one state to give rise to the calculated ΔC_p values.[31] Our MD simulations with ScNreA not only provide evidence for such conjectures from the experimental data but also capture new elements beyond the X-ray crystal structures.

The repeated entry and exit events observed in the MD simulations reveal gating of anion entry through electropositive sidechains and final anion coordination to amide backbones and the key tryptophan at position 45. Throughout the trajectories, water molecules are dynamic and can penetrate the binding pocket, mediating transient interactions with the bound anion. We speculate this solvation can also be a competitive process, allowing for anion release into bulk water. Overall, local motions across flexible loops are responsive to anion binding. These are distinct and occur to varying degrees for each anion but are globally subtle. Perhaps this is unsurprising given that ScNreA is a compact sensory protein with a GAF domain fold for a low molecular weight inorganic anion.

Across our observations, we also considered how the physical differences between each anion could contribute. When comparing all three anions, no clear correlation can be drawn. However, this is not the case if we look to the native nitrate and nitrite. While both anions are monoanionic, relative to nitrite, nitrate is a weak conjugate base (pK_b: 14 versus 9.5) with a smaller ionic radius (179 versus 192 pm) and lower dehydration enthalpy (310 versus 410 kJ/mol).[40,41] Anion shape could also play a role. The underlying promiscuity of ScNreA cannot be distilled to a single physical property. This is not to say that ScNreA can recognize

any anion, whether native or non-native, but rather that its selectivity is on a spectrum to meet its physiological function as nitrate sensor. We believe that such a conclusion is an inherent supramolecular feature of nitrate, and perhaps, anion binding proteins in general, that Nature has adapted for anion coordination chemistry.

Supporting Information

Experimental methods, data analysis, and supporting data (PDF). Supporting movies for the MD simulations (MPG).

Author Contributions

S.C.D. designed and supervised the research project with contributions from S.O.N. for MD simulations and G.M. for stopped-flow kinetic experiments. K.J. carried out ITC experiments, MD simulations, stopped-flow kinetic experiments, and data analysis. E.K.P. and C.M. carried out stopped-flow kinetic experiments and data analysis. K.A.A. contributed expertise for analysis of the MD simulations. S.A., R.L.E.V., and H.G. contributed expertise for the stopped-flow kinetic experiments. K.J. and S.C.D. wrote the manuscript with input from all the authors.

Acknowledgements

High-performance computing resources were provided by the Texas Advanced Computing Center (TACC) at the University of Texas at Austin (http://www.tacc.utexas.edu). Research support was provided to S.C.D. by UT Dallas, the Welch Foundation (AT-1918-20170325, AT-2060-20210327, AT-2060-20240404), and the National Institute of General Medical Sciences of the National Institutes of Health (R35GM128923); G.M. by the Robert A. Welch Foundation (AT-2073-20210327), the National Institute of General Medical Sciences of the National Institutes of Health (R35GM128704), and the National Science Foundation (CHE-2045984). This study does not represent the views of the supporting agencies and is the responsibility of the authors.

Conflicts of Interest

There are no conflicts to declare.

Data Availability Statement

The data that support the findings of this study are available in the main text and supplementary material of this article. The corresponding authors can be contacted for additional requests.

Figures and Tables

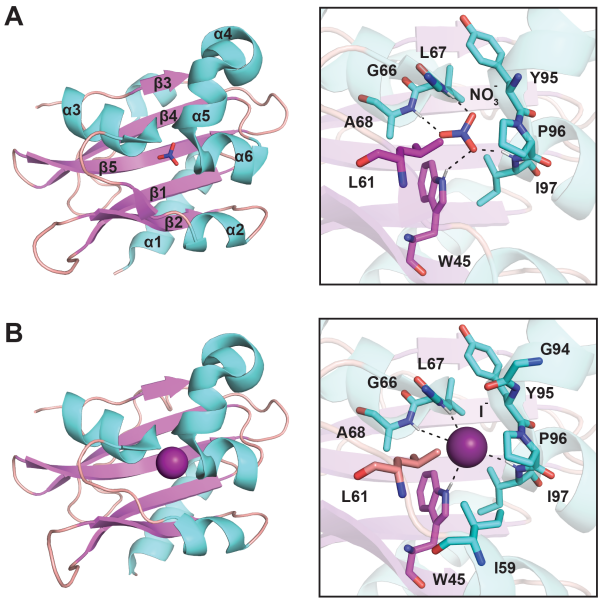

Figure 1. X-ray crystal structure of (A) nitrate bound (PDB: 4IUK) and (B) iodide bound (PDB ID: 4IUH) NreA from *Staphylococcus carnosus* (ScNreA). The residues within 4 Å of nitrate and 5 Å of iodide are shown. All residues are labeled with the single letter amino acid code and position number. The colors of the residues correspond to the secondary structure as follows: alpha helix (turquoise), beta sheet (magenta), and flexible loop (pale salmon).

Table 1. [a]Thermodynamic Parameters of Anion Binding to ScNreA from 10–25 °C.

Anion	Temperature (°C)	K_d (μM)	ΔH (kJ/mol)	TΔS (kJ/mol)	ΔG (kJ/mol)	ΔC_p (J/mol•K)
Nitrate	25	4.0 ± 0.1	-32.1 ± 0.1	-1.4 ± 0.1	-30.8 ± 0.0	-308.2 ± 21.6
	20	2.7 ± 0.1	-30.1 ± 0.1	1.3 ± 0.1	-31.3 ± 0.1	
	15	2.5 ± 0.2	-28.4 ± 0.1	2.6 ± 0.1	-31.0 ± 0.2	
	10	1.4 ± 0.1	-27.0 ± 0.1	4.8 ± 0.4	-31.7 ± 0.3	
Iodide	25	44.5 ± 2.0	-21.5 ± 0.3	3.3 ± 0.1	-24.9 ± 0.1	242.3 ± 34.9
	20	37.7 ± 0.8	-22.5 ± 0.0	2.4 ± 0.1	-24.9 ± 0.1	
	15	34.7 ± 0.0	-23.5 ± 0.3	1.1 ± 0.3	-24.6 ± 0.0	
	10	26.6 ± 3.7	-24.7 ± 0.4	0.2 ± 0.0	-24.9 ± 0.4	
Nitrite	25	109 ± 11	-17.8 ± 0.0	4.8 ± 0.3	-22.6 ± 0.4	33.1 ± 11.2
	20	97.5 ± 10.6	-18.0 ± 0.1	4.6 ± 0.2	-22.5 ± 0.3	
	15	85.3 ± 5.9	-18.1 ± 0.1	4.4 ± 0.1	-22.5 ± 0.2	
	10	71.8 ± 6.7	-18.3 ± 0.3	4.1 ± 0.2	-22.5 ± 0.1	

[a]The best-fit values for each parameter were obtained through a global analysis of three technical measurements for two biological replicates and are reported as the average with standard deviation. The protein and anion samples were prepared in 50 mm HEPES buffer with 50 mM sodium chloride at pH 7.8.

Table 2. [a]Kinetic Parameters of Anion Binding to ScNreA at 10 °C.

Anion	k_{on} (× 10^5) ($M^{-1}s^{-1}$)	k_{off} (s^{-1})
Nitrate	2.70 ± 0.01	3.26 ± 0.49
Iodide	2.45 ± 0.01	12.32 ± 1.06
Nitrite	1.82 ± 0.01	21.39 ± 2.26

[a]The kinetic parameters from three technical measurements for two biological replicates are reported as the average with propagated standard deviation. The protein and anion samples were prepared in 50 mm HEPES buffer with 50 mM sodium chloride at pH 7.8.

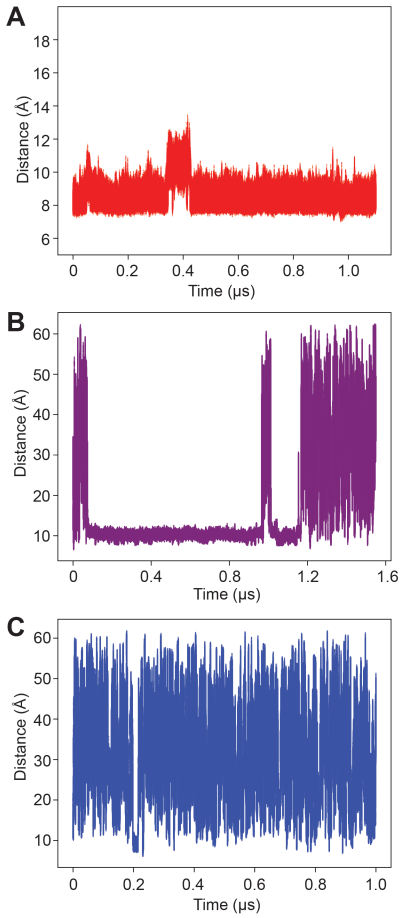

Figure 2. Molecular dynamics (MD) simulations capture the anion binding plasticity of ScNreA. Distances between the alpha carbon (Cα) of residue W45 to the center of mass of (A) nitrate, (B) iodide, and (C) nitrite are shown as a function of time from a representative trajectory (Figure S19).

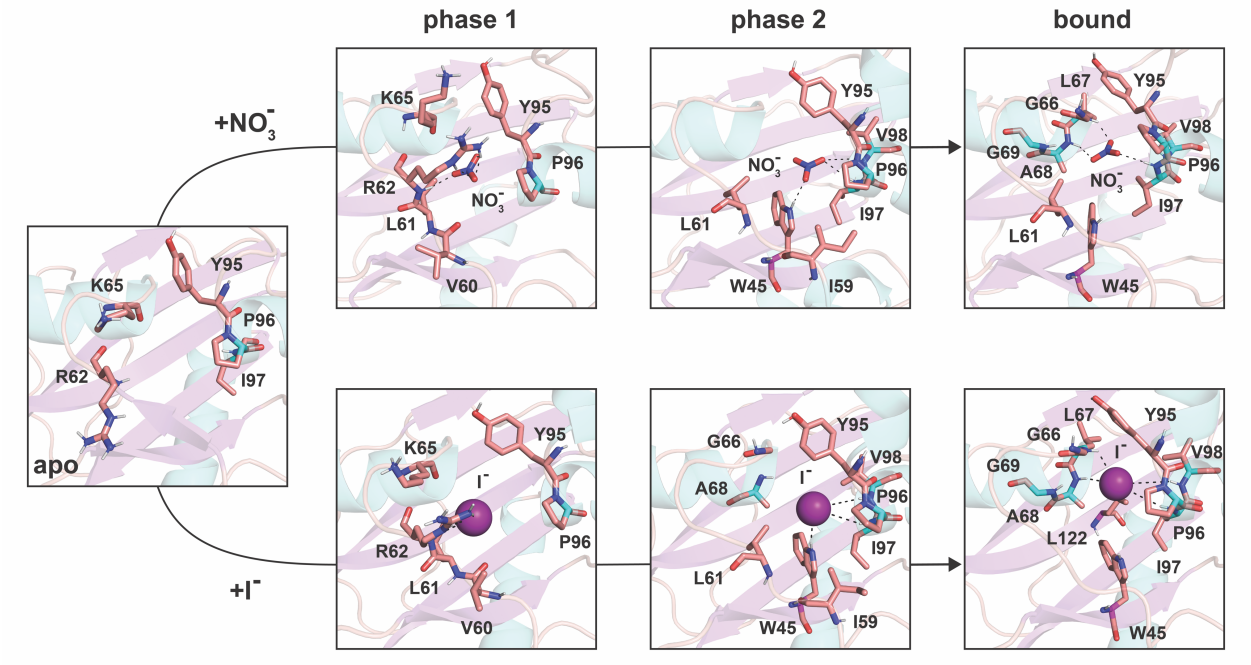

Figure 3. MD simulations reveal an anion entry pathway from bulk water into the ScNreA binding pocket. Representative snapshots of the apo, intermediate, and bound phases for nitrate and iodide are shown from left to right. Possible interactions between ScNreA and the bound anions are shown as dashed lines. Residues within 4 Å of nitrate and 5 Å of iodide are shown as sticks with the single letter amino acid code and position number.

References

[1] Z. Wang, P. A. Cole, in *Protein Kinase Inhib. Res. Med.* (Ed.: K.M.B.T.-M. in E. Shokat), Academic Press, **2014**, pp. 1–21.
[2] M. J. Langton, C. J. Serpell, P. D. Beer, *Angew. Chemie Int. Ed.* **2016**, *55*, 1974–1987.
[3] S. K. Raut, K. Singh, S. Sanghvi, V. Loyo-Celis, L. Varghese, E. R. Singh, S. Gururaja Rao, H. Singh, *Biosci. Rep.* **2024**, *44*, BSR20240029.
[4] J. W. Steed, J. L. Atwood, in *Supramol. Chem.*, John Wiley & Sons, Inc., Chichester, West Sussex, **2022**, pp. 265–350.
[5] E. M. Wright, J. M. Diamond, *Physiol. Rev.* **1977**, *57*, 109–156.
[6] D. M. Lawson, C. E. Williams, L. A. Mitchenall, R. N. Pau, *Structure* **1998**, *6*, 1529–1539.
[7] M. Elias, A. Wellner, K. Goldin-Azulay, E. Chabriere, J. A. Vorholt, T. J. Erb, D. S. Tawfik, *Nature* **2012**, *491*, 134–137.
[8] F. A. Quiocho, *Kidney Int.* **1996**, *49*, 943–946.
[9] T. T. Waldron, M. A. Modestou, K. P. Murphy, *Protein Sci.* **2003**, *12*, 871–874.
[10] G. De Simone, C. T. Supuran, *J. Inorg. Biochem.* **2012**, *111*, 117–129.
[11] L. Lagostena, G. Zifarelli, A. Picollo, *J. Am. Soc. Nephrol.* **2019**, *30*, 293–302.
[12] J. N. Tutol, H. C. Kam, S. C. Dodani, *ChemBioChem* **2019**, *20*, 1759–1765.
[13] J. N. Tutol, W. Peng, S. C. Dodani, *Biochemistry* **2019**, *58*, 31–35.
[14] W. Peng, C. C. Maydew, H. Kam, J. K. Lynd, J. N. Tutol, S. M. Phelps, S. Abeyrathna, G. Meloni, S. C. Dodani, *Chem. Sci.* **2022**, *13*, 12659–12672.
[15] W. S. Y. Ong, K. Ji, V. Pathiranage, C. Maydew, K. Baek, R. L. E. Villones, G. Meloni, A. R. Walker, S. C. Dodani, *Angew. Chemie Int. Ed.* **2023**, *62*, e202302304.
[16] J. N. Tutol, W. S. Y. Ong, S. M. Phelps, W. Peng, H. Goenawan, S. C. Dodani, *ACS Cent. Sci.* **2024**, *10*, 77–86.
[17] K. Ji, K. Baek, W. Peng, K. A. Alberto, H. Torabifard, S. O. Nielsen, S. C. Dodani, *Chem. Commun.* **2022**, *58*, 965–968.
[18] K. H. SCHLEIFER, U. FISCHER, *Int. J. Syst. Bacteriol.* **1982**, *32*, 153–156.
[19] S. Nilkens, M. Koch‐Singenstreu, V. Niemann, F. Götz, T. Stehle, G. Unden, *Mol. Microbiol.* **2014**, *91*, 381–393.
[20] V. Niemann, M. Koch-Singenstreu, A. Neu, S. Nilkens, F. Götz, G. Unden, T. Stehle, *J. Mol. Biol.* **2014**, *426*, 1539–1553.
[21] I. Fedtke, A. Kamps, B. Krismer, F. Götz, *J. Bacteriol.* **2002**, *184*, 6624–6634.
[22] S. Durand, M. Guillier, *Front. Mol. Biosci.* **2021**, *8*, 667758.
[23] R. Klein, A. Kretzschmar, G. Unden, *Mol. Microbiol.* **2020**, *113*, 369–380.
[24] J. M. Fox, M. Zhao, M. J. Fink, K. Kang, G. M. Whitesides, *Annu. Rev. Biophys.* **2018**, *47*, 223–250.
[25] X. Du, Y. Li, Y.-L. Xia, S.-M. Ai, J. Liang, P. Sang, X.-L. Ji, S.-Q. Liu, *Int. J. Mol. Sci.* **2016**, *17*, 144.
[26] K. P. Murphy, E. Freire, Y. Paterson, *Proteins Struct. Funct. Bioinforma.* **1995**, *21*, 83–90.
[27] S. P. Edgcomb, B. M. Baker, K. P. Murphy, *Protein Sci.* **2000**, *9*, 927–933.
[28] J. P. Robblee, W. Cao, A. Henn, D. E. Hannemann, E. M. De La Cruz, *Biochemistry* **2005**, *44*, 10238–10249.
[29] J. L. Fulton, G. K. Schenter, M. D. Baer, C. J. Mundy, L. X. Dang, M. Balasubramanian, *J. Phys. Chem. B* **2010**, *114*, 12926–12937.
[30] M. Antalek, E. Pace, B. Hedman, K. O. Hodgson, G. Chillemi, M. Benfatto, R. Sarangi,

P. Frank, *J. Chem. Phys.* **2016**, *145*, 044318.
[31] S. Vega, O. Abian, A. Velazquez-Campoy, *Biochim. Biophys. Acta - Gen. Subj.* **2016**, *1860*, 868–878.
[32] B. F. Peterman, K. J. Laidler, *Biochim. Biophys. Acta - Protein Struct.* **1979**, *577*, 314–323.
[33] S. R. J. Hoare, in *Assay Guid. Man.* (Eds.: S. Markossian, A. Grossman, K. Brimacombe Michelle Arkin, D. Auld, C. Austin, J.D. Baell Thomas Chung, N.P. Coussens, J.L. Dahlin Viswanath Devanarayan, T.L. Foley, M. Glicksman Kirill Gorshkov, J. V Haas, M.D. Hall, S. Hoare James Inglese, P.W. Iversen, S.C. Kales, M. Lal-Nag Zhuyin Li, J. McGee, O. McManus, T. Riss Peter Saradjian, G. Sitta Sittampalam, M.O. Tarselli Joseph Trask, Y. Wang, J.R. Weidner Mary Jo Wildey, K. Wilson, M. Xia, X. Xu), Eli Lilly & Company And The National Center For Advancing Translational Sciences, Bethesda, MD USA, **2021**, pp. 41–80.
[34] J. C. Phillips, D. J. Hardy, J. D. C. Maia, J. E. Stone, J. V. Ribeiro, R. C. Bernardi, R. Buch, G. Fiorin, J. Hénin, W. Jiang, R. McGreevy, M. C. R. Melo, B. K. Radak, R. D. Skeel, A. Singharoy, Y. Wang, B. Roux, A. Aksimentiev, Z. Luthey-Schulten, L. V. Kalé, K. Schulten, C. Chipot, E. Tajkhorshid, *J. Chem. Phys.* **2020**, *153*, 044130.
[35] N. Michaud‐Agrawal, E. J. Denning, T. B. Woolf, O. Beckstein, *J. Comput. Chem.* **2011**, *32*, 2319–2327.
[36] R. Gowers, M. Linke, J. Barnoud, T. Reddy, M. Melo, S. Seyler, J. Domański, D. Dotson, S. Buchoux, I. Kenney, O. Beckstein, in *Proc. 15th Python Sci. Conf.* (Eds.: S. Benthall, S. Rostrup), **2016**, pp. 98–105.
[37] P. H. Hünenberger, A. E. Mark, W. F. van Gunsteren, *J. Mol. Biol.* **1995**, *252*, 492–503.
[38] W. Humphrey, A. Dalke, K. Schulten, *J. Mol. Graph.* **1996**, *14*, 33–38.
[39] C. C. David, D. J. Jacobs, in *Protein Dyn.* (Ed.: D.R. Livesay), Humana Press, Totowa, NJ, **2014**, pp. 193–226.
[40] Y. Marcus, *Biophys. Chem.* **1994**, *51*, 111–127.
[41] A. K. SenGupta, in *Ion Exch. Environ. Process.*, John Wiley & Sons, Inc., **2017**, pp. 461–462.